Fractal measures and their singularities: The characterization of strange sets

Thomas C. Halsey, Mogens H. Jensen, Leo P. Kadanoff, Itamar Procaccia,* and Boris I. Shraiman†
The James Franck Institute, The Enrico Fermi Institute for Nuclear Studies, and Department of Chemistry, The University of Chicago, 5640 South Ellis Avenue, Chicago, Illinois 60637
(Received 26 August 1985)

We propose a description of normalized distributions (measures) lying upon possibly fractal sets; for example those arising in dynamical systems theory. We focus upon the scaling properties of such measures, by considering their singularities, which are characterized by two indices: α, which determines the strength of their singularities; and f, which describes how densely they are distributed. The spectrum of singularities is described by giving the possible range of α values and the function $f(\alpha)$. We apply this formalism to the 2^∞ cycle of period doubling, to the devil's staircase of mode locking, and to trajectories on 2-tori with golden-mean winding numbers. In all cases the new formalism allows an introduction of smooth functions to characterize the measures. We believe that this formalism is readily applicable to experiments and should result in new tests of global universality.

I. INTRODUCTION

Nonlinear physics presents us with a perplexing variety of complicated fractal objects and strange sets. Notable examples include strange attractors for chaotic dynamical systems,[1,2] configurations of Ising spins at critical points,[3] the region of high vorticity in fully developed turbulence,[4,5] percolating clusters and their backbones,[6] and diffusion-limited aggregates.[7,8] Naturally one wishes to characterize the objects and describe the events occurring on them. For example, in dynamical systems theory one is often interested in a strange attractor (the object) and how often a given region of the attractor is visited (the event). In diffusion-limited aggregation, one is interested in the probability of a random walker landing next to a given site on the aggregate.[8] In percolation, one may be interested in the distribution of voltages across the different elements in a random-resistor network.[6]

In general, one can describe such events by dividing the object into pieces labeled by an index i which runs from 1 up to N. The size of the ith piece is l_i and the event occurring upon it is described by a number M_i. For example, in critical phenomena, we can let M_i be the magnetization of the region labeled by i. Such a picture is natural in the droplet theory of the Ising model, where one argues that if the region i has a size of order l, the magnetization has a value of the order of

$$M_i \sim l^y , \tag{1.1}$$

where y (or y_σ) is one of the standard critical indices.[9] Since these droplets are imagined to fill the entire space, the density of such droplets is simply

$$\rho(l) \sim \frac{1}{l^d} , \tag{1.2}$$

where d is the Euclidean dimension of space. In fact, in critical phenomena we define a whole sequence of y_q's by saying that the typical values of $(M_i)^q$ vary with q and have the form[10]

$$(M_i)^q \sim l^{y_q}, \quad q=1,2,3,\ldots . \tag{1.3}$$

Typically, our attention focuses upon the values of y_q that are greater than zero and *we have only a few distinct values of these.*[11]

In this paper we are interested not in critical phenomena but instead in a broad class of strange objects. However, we specialize our treatment to the case in which M_i has the meaning of a probability that some event will occur upon the ith piece. For example, in experiments on chaotic systems one measures a time series $\{\mathbf{x}_i\}_{i=1}^N$. These points belong to a trajectory in some d-dimensional phase space. Typically, the trajectory does not fill the d-dimensional space even when $N\to\infty$, because the trajectory lies on a strange attractor of dimension D, $D<d$. One can ask now how many times, N_i, the time series visits the ith box. Defining $p_i=\lim_{N\to\infty}(N_i/N)$, we generate the measure on the attractor $d\mu(\mathbf{x})$, because

$$p_i = \int_{i\text{th box}} d\mu(\mathbf{x}) .$$

In many nonlinear problems, the possible scaling behavior is richer and more complex than is the case in critical phenomena. If a scaling exponent α is defined by saying that

$$p_i^q \sim l_i^{\alpha q} , \tag{1.4}$$

then α [roughly equivalent to y_q/q in Eq. (1.3)] can take on a range of values, corresponding to different regions of the measure. In particular, if the system is divided into pieces of size l, we suggest that the number of times α takes on a value between α' and $\alpha'+d\alpha'$ will be of the form

$$d\alpha' \rho(\alpha') l^{-f(\alpha')} , \tag{1.5}$$

where $f(\alpha')$ is a continuous function. The exponent $f(\alpha')$ reflects the differing dimensions of the sets upon which the singularities of strength α' may lie. This expression is roughly equivalent to Eq. (1.2), except that now, instead of the dimension d, we have a fractal dimension $f(\alpha)$

 ©1986 The American Physical Society

which varies with α. Thus, we model fractal measures by interwoven sets of singularities of strength α, each characterized by its own dimension $f(\alpha)$. The rest of our formalism attempts to unravel this complexity in a workable fashion.

The concept of a singularity strength α was stressed in the context of diffusion-limited aggregation in independent work of Turkevich and Scher[12] and of Halsey, Meakin, and Procaccia.[8] The latter group pointed out the significance of the density of singularities and expressed it in terms of f.

In order to determine the function $f(\alpha)$ for a given measure, we must relate it to observable properties of the measure. We relate $f(\alpha)$ to a set of dimensions which have been introduced by Hentschel and Procaccia, the set D_q defined by[13]

$$D_q=\lim_{l\to 0}\left[\frac{1}{q-1}\frac{\ln\chi(q)}{\ln l}\right], \tag{1.6}$$

where

$$\chi(q)=\sum_i p_i^q . \tag{1.7}$$

D_0 is just the fractal dimension of the support of the measure, while D_1 is the information dimension and D_2 is the correlation dimension.[14]

As q is varied in Eq. (1.7), different subsets, which are associated with different scaling indices, become dominant. Substituting Eqs. (1.4) and (1.5) into Eq. (1.7), we obtain

$$\chi(q)=\int d\alpha'\rho(\alpha')l^{-f(\alpha')}l^{q\alpha'} . \tag{1.8}$$

Since l is very small, the integral in Eq. (1.8) will be dominated by the value of α' which makes $q\alpha'-f(\alpha')$ smallest, provided that $\rho(\alpha')$ is nonzero. Thus, we replace α' by $\alpha(q)$, which is defined by the extremal condition

$$\frac{d}{d\alpha'}[q\alpha'-f(\alpha')]\bigg|_{\alpha'=\alpha(q)}=0 .$$

We also have

$$\frac{d^2}{d(\alpha')^2}[q\alpha'-f(\alpha')]\bigg|_{\alpha'=\alpha(q)}>0 ,$$

so that

$$f'(\alpha(q))=q , \tag{1.9a}$$

$$f''(\alpha(q))<0 . \tag{1.9b}$$

It then follows from Eq. (1.6) that[8]

$$D_q=\frac{1}{q-1}[q\alpha(q)-f(\alpha(q))] . \tag{1.10}$$

Thus, if we know $f(\alpha)$, and the spectrum of α values, we can find D_q. Alternatively, given D_q, we can find $\alpha(q)$ since

$$\alpha(q)=\frac{d}{dq}[(q-1)D_q] , \tag{1.11}$$

and, knowing $\alpha(q)$, $f(q)$ can be obtained from Eq. (1.10).

Equations (1.9)–(1.11) are the main formal results used in this paper. In the next section we develop the formalism outlined here in somewhat more detail and apply it to systems with strong self-similarity properties. In Sec. III we apply the formalism to some important examples of measures arising in dynamical systems. We examine the 2^∞ cycle of period doubling,[15] the devil's staircase of mode locking in circle maps,[16,17] and the elements of the critical cycle at the onset of chaos in circle maps with golden-mean winding number.[18–20] Although all of these cases have been examined previously, we are able to find a *smooth* function with which to characterize them. Furthermore, these characterizations are universal. Other attempts to study these measures have led to nowhere smooth scaling functions.[15,21] Since the characterizations are functions rather than numbers, they offer much more information than fractal dimensions. Unlike power spectra, these functions possess an immediate connection to the metric properties of the measures involved, and do not call for cumbersome interpretation. Therefore, we believe that experimental measurements of D_q, and thus of $f(\alpha)$, should replace more common tests of universality in the transition to chaos. We give many examples of the procedures employed, and we hope to encourage experiments to follow these lines.

II. EXACTLY SOLUBLE STRANGE SETS

A. Preliminaries

We begin by introducing a more general definition of the dimensions D_q. Consider a strange set S embedded in a finite portion of d-dimensional Euclidean space. Imagine partitioning the set into some number of disjoint pieces, $S_1, S_2, \ldots, S_N$, in which each piece has a measure p_i and lies within a ball of radius l_i, where each l_i is restricted by $l_i<l$. Then define a partition function

$$\Gamma(q,\tau,\{S_i\},l)=\sum_{i=1}^{N}\frac{p_i^q}{l_i^\tau} . \tag{2.1}$$

Eventually we shall argue that, for large N, this partition function is of the order unity only when

$$\tau=(q-1)D_q . \tag{2.2}$$

To make this argument, consider now two regions:

$$\text{region } A:\ q\geq 1,\ \tau\geq 0 , \tag{2.3a}$$

$$\text{region } B:\ q\leq 1,\ \tau\leq 0 . \tag{2.3b}$$

In region A, adjust the partition $\{S_i\}$ so as to maximize Γ. In region B, adjust it so that Γ is as small as possible. Then define

$$\Gamma(q,\tau,l)=\text{Sup }\Gamma(q,\tau,\{S_i\},l)\ \ (\text{region } A) , \tag{2.4a}$$

$$\Gamma(q,\tau,l)=\text{Inf }\Gamma(q,\tau,\{S_i\},l)\ \ (\text{region } B) . \tag{2.4b}$$

The supremum in region A will exist as long as there are constants $a>0$ and $\alpha_0>0$, so that for any possible subset of S, $\{S_i\}$, we have

$$p_i\leq a(l_i)^{\alpha_0} . \tag{2.5}$$

Then $\Gamma(q,\tau,l)$ will exist and be less than infinity whenever

$$\alpha_0(q-1)>\tau\ . \tag{2.6}$$

Next define

$$\Gamma(q,\tau)=\lim_{l\to 0}[\Gamma(q,\tau,l)]\ . \tag{2.7}$$

Notice that $\Gamma(q,\tau)$ is a monotone nondecreasing function of τ and a monotone nonincreasing function of q. One can argue that there is a unique function $\tau(q)$ such that

$$\Gamma(q,\tau)=\begin{cases}\infty & \text{for } \tau>\tau(q),\\ 0 & \text{for } \tau<\tau(q)\ .\end{cases} \tag{2.8}$$

Equation (2.8) permits us to define D_q as

$$(q-1)D_q=\tau(q)\ . \tag{2.9}$$

Once D_q is known, Eqs. (1.10) and (1.11) will then give $\alpha(q)$ and $f(q)$. Notice that our definition of D_q is precisely the one which makes D_0 the Hausdorff dimension.

B. Connection to previously defined D_q

Hentschel and Procaccia[13] also defined a D_q, which we now denote as $D_q^{\rm HP}$. To relate the two quantities, recall that the authors of Ref. 13 defined a partition in which all the diameters l_i had the same value l. We know that

$$\Gamma(q,\tau,l)\begin{cases}>l^{-\tau}\displaystyle\sum_{i=1}^{N}p_i^q & \text{(region } A\text{)}\\ <l^{-\tau}\displaystyle\sum_{i=1}^{N}p_i^q & \text{(region } B\text{)}\ .\end{cases} \tag{2.10}$$

If τ is chosen correctly, i.e., $\tau=\tau(q)$, the left-hand side of Eq. (2.10) will neither go to zero nor diverge very strongly as $l\to 0$. In particular, we guess that $\Gamma(l)$ is no worse than logarithmically dependent upon these quantities. Then

$$\lim_{l\to 0}[\ln\Gamma(q,\tau(q),l)/\ln l]\to 0\ .$$

We have now

$$\frac{\tau}{q-1}\le\lim_{l\to 0}\left\{\frac{\ln\left[\displaystyle\sum_{i=1}^{N}p_i^q\right]}{(\ln l)(q-1)}\right\}\ . \tag{2.11}$$

The right-hand side of (2.11) is $D_q^{\rm HP}$. We thus find

$$D_q\le D_q^{\rm HP}\ . \tag{2.12}$$

Since we believe that Eq. (2.10) will often be an order of magnitude equality when $\tau=\tau(q)$, we think that Eq. (2.12) will be an equality in most cases of interest.

At this point we turn to some simple examples to illustrate the quantities $\tau(q)$. These examples will enable us to gain intuition about the quantities $\alpha(q)$ and $f(\alpha)$.

C. Exactly soluble examples

1. Power-law singularity

One of the simplest possible applications of this formalism is to a probability measure with only one power-law singularity. Imagine a probability density $\rho(x)=\tilde{\alpha}x^{\tilde{\alpha}-1}$ on $x\in[0,1]$, where $0<\tilde{\alpha}<1$. Let us partition the interval into N segments $[x_i, x_i+\Delta x]$, with $\Delta x=N^{-1}$. The total probability measure on all of these intervals except for that adjoining zero is well approximated by $\rho(x_i)\Delta x$. The probability upon the segment adjoining zero possesses a probability $p_0=(\Delta x)^{\tilde{\alpha}}$. The partition function is therefore

$$\Gamma(q,\tau,\Delta x)\approx\frac{(\Delta x)^{\tilde{\alpha}q}}{(\Delta x)^{\tau}}+\sum_{i\neq 0}\frac{\tilde{\alpha}x_i^{\tilde{\alpha}-1}(\Delta x)^q}{(\Delta x)^{\tau}}\ . \tag{2.13}$$

There are $(\Delta x)^{-1}$ terms in the sum, so that

$$\Gamma(q,\tau,\Delta x)\sim(\Delta x)^{\tilde{\alpha}q-\tau}+(\Delta x)^{q-1-\tau}\ . \tag{2.14}$$

Thus, since we require that Γ neither go to zero nor infinity, we have that

$$\tau=\min\{q-1,\tilde{\alpha}q\}\ , \tag{2.15a}$$

or

$$D_q=\frac{1}{q-1}\min\{q-1,\tilde{\alpha}q\}\ . \tag{2.15b}$$

Thus for $q>q^*=1/(1-\tilde{\alpha})$, the dimensions correspond to a value of $\alpha=\tilde{\alpha}$ and of $f=0$, while for $q<q^*$ the dimensions correspond to $\alpha=1$ and $f=1$. Thus, in this example the f-α spectrum consists of two points, corresponding to the two types of behavior in the measure.

2. Cantor sets and generators

If a measure possesses an exact recursive structure, one can find its D_q. Suppose that the measure can be generated by the following process. Start with the original region which has measure 1 and size 1. Divide the region into pieces S_i, $i=1,2,\ldots,N$, with measure p_i and size l_i. Suppose that the maximum of l_i is given by l. Then at the first stage we can construct a partition function,

$$\Gamma(q,\tau,l)=\sum_i\frac{p_i^q}{l_i^{\tau}}\ . \tag{2.16}$$

Continue the Cantor construction. At the next stage each piece of the set is further divided into N pieces, each with a measure reduced by a factor p_j and size by a factor l_j. At this level the partition function will be

$$\Gamma(q,\tau,l^2)=[\Gamma(q,\tau,l)]^2\ . \tag{2.17}$$

We see at once that, for this kind of measure, the first partition function $\Gamma(l)$ will generate all the others, and that $\tau(q)$ is defined by

$$\Gamma(q,\tau(q),l)=1\ . \tag{2.18}$$

If a partition with finite N yields a Γ which obeys (2.17), that partition is called a generator.[22]

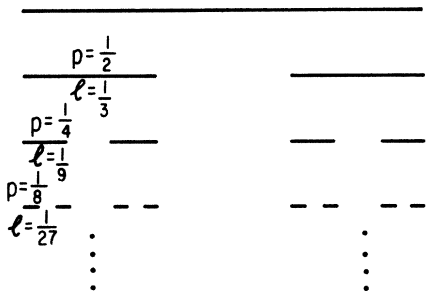

FIG. 1. The construction of the uniform Cantor set. At each stage of the construction the central third of each segment is removed from the set. Each segment has measure $p_0=(\frac{1}{2})^n$ and scale $l_0=(\frac{1}{3})^n$, where n is the number of generations.

3. *Uniform Cantor set*

A simple example is the classical Cantor set obtained by dividing the interval [0,1] as shown in Fig. 1. We initially replace the unit interval with two intervals, each of length $l=\frac{1}{3}$. Each of these intervals receives the same measure $p=\frac{1}{2}$. At the next stage of the construction of the measure this same process is repeated on each of these two intervals. Thus, for this measure we require

$$2\left[\frac{(\frac{1}{2})^q}{(\frac{1}{3})^\tau}\right]=1\ , \tag{2.19}$$

which yields

$$\tau=(q-1)[\ln(2)/\ln(3)]\ \ [\text{or } D_q=\ln(2)/\ln(3)]\ . \tag{2.20}$$

If l_0 is the length scale of the intervals at a particular level of the partitioning, and p_0 is the measure for such an interval, then

$$p_0=l_0^{\ln(2)/\ln(3)}\ . \tag{2.21}$$

Calling the index of the singularity α, i.e., $p_0\sim l_0^\alpha$, we have here $\alpha=\ln(2)/\ln(3)$. If we further ask what is the density of these singularities, we find immediately that it is simply the density of the set,

$$\rho(l_0)=\frac{1}{l_0^{\ln(2)/\ln(3)}}\ , \tag{2.22}$$

and Eq. (1.5) leads to $f=\ln(2)/\ln(3)$. Thus in this example, $\alpha=f$, and also

$$\tau(q)=q\alpha-f\ . \tag{2.23}$$

Although Eq. (2.23) is trivial here, we shall see that its analog, Eq. (1.10), also holds in the most general cases.

4. *Two-scale Cantor set*

A somewhat less trivial example is obtained by constructing a Cantor set as in Fig. 2. Here we use two rescaling parameters l_1 and l_2 and two measures p_1 and p_2, and then continue to subdivide self-similarly. We assume that $l_2>l_1$. It is apparent that this example also has a generator, since the condition

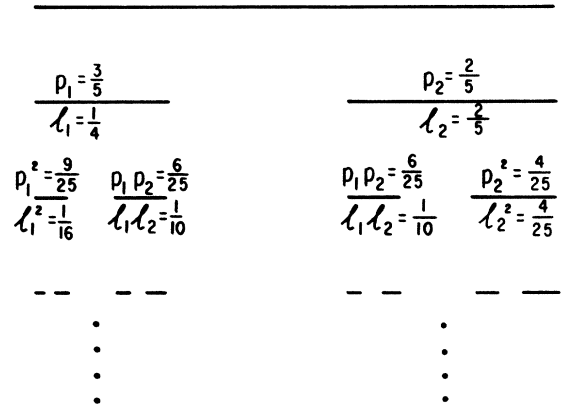

FIG. 2. A Cantor-set construction with two rescalings $l_1=0.25$ and $l_2=0.4$ and respective measure rescalings $p_1=0.6$ and $p_2=0.4$. The division of the set continues self-similarly.

$$\Gamma(q,\tau,l_2^n)=\left[\frac{p_1^q}{l_1^\tau}+\frac{p_2^q}{l_2^\tau}\right]^n=1 \tag{2.24}$$

results in a τ that does not depend on n. The value of τ depends, however, on q. In Fig. 3 we show $D_q=\tau(q)/(q-1)$ as a function of q, as obtained numerically by solving Eq. (2.24). To further understand this curve, we can examine the quantity $\Gamma(l_2^n)$ for this case explicitly:

$$\Gamma(q,\tau,l_2^n)=\sum_m\binom{n}{m}p_1^{mq}p_2^{(n-m)q}(l_1^m l_2^{n-m})^{-\tau}=1\ . \tag{2.25}$$

We expect that in the limit $n\to\infty$ the largest term in this sum should dominate. To find the largest term we compute

$$\frac{\partial\ln\Gamma(l_2^n)}{\partial m}=0\ . \tag{2.26}$$

Using the Stirling approximation, we find that Eq. (2.26) is equivalent to

$$\tau=\frac{\ln(n/m-1)+q\ln(p_1/p_2)}{\ln(l_1/l_2)}\ . \tag{2.27}$$

Since we expect that the maximal term dominates the sum, we have a second equation,

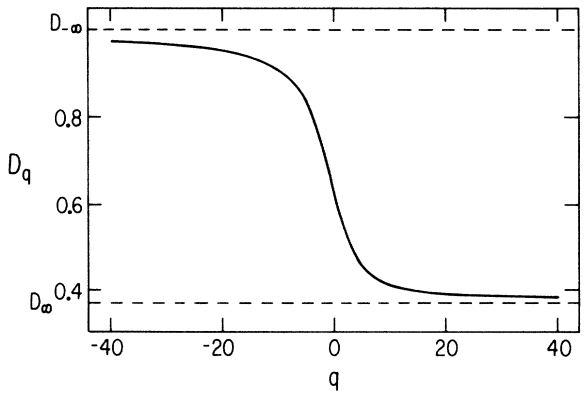

FIG. 3. D_q plotted vs q for the two-scale Cantor set of Fig. 2.

$$\binom{n}{m} p_1^{mq} p_2^{(n-m)} \left[\frac{1}{l_1^m l_2^{(n-m)}} \right]^{\tau} = 1 . \tag{2.28}$$

Inserting Eq. (2.27) into Eq. (2.28) leads to an equation for n/m. After some algebraic manipulation, one finds

$$\ln(n/m)\ln(l_1/l_2) - \ln(n/m-1)\ln l_1 = q(\ln p_1 \ln l_2 - \ln p_2 \ln l_1) . \tag{2.29}$$

We thus see that for any given q there will be a value of n/m which solves Eq. (2.29) and, in turn, determines τ from Eq. (2.27). This maximal term which determines τ actually comes from a set of $\binom{n}{m}$ segments, all of which have the same size $l_1^m l_2^{(n-m)}$. Their density exponent f is determined by

$$\binom{n}{m} (l_1^m l_2^{(n-m)})^f = 1 , \tag{2.30}$$

or

$$f = \frac{(n/m-1)\ln(n/m-1) - (n/m)\ln(n/m)}{\ln l_1 + (n/m-1)\ln l_2} . \tag{2.31}$$

The exponent determining the singularity in the measure, α, is determined by

$$p_1^m p_2^{(n-m)} = (l_1^m l_2^{(n-m)})^{\alpha} , \tag{2.32}$$

or

$$\alpha = \frac{\ln p_1 + (n/m-1)\ln p_2}{\ln l_1 + (n/m-1)\ln l_2} . \tag{2.33}$$

Thus, for any chosen q, the measure scales as $\alpha(q)$ on a set of segments which converge to a set of dimension $f(q)$. As q is varied, different regions of the set determine D_q. It can be shown that Eqs. (2.27), (2.29), (2.31), and (2.33) again lead to

$$\tau = (q-1)D_q = q\alpha(q) - f(q) . \tag{2.34}$$

We can also understand the spectrum of scaling indices α by considering the "kneading sequences" for the segments. In the first level of the construction there are two segments of sizes l_1 and l_2 and measures p_1 and p_2 which we can label L (left) and R (right). At the next level we have four segments, which we can reach by going left or right: LL, LR, RL, and RR. Thus the measure and the size of any segment are determined by its address, the kneading sequence of L's and R's. For example, the size of a segment is $l_1^m l_2^{(n-m)}$, where m and $n-m$ are, respectively, the numbers of L's and R's in the kneading sequence. Clearly, the sequence $LLL\ldots LLL\ldots$ is associated with $\alpha = \ln(p_1)/\ln(l_1) = D_{\infty}$, which lies on the edge of the spectrum, while the sequence $RRR\ldots RRR\ldots$ is associated with the singularity lying on the other edge of the spectrum. Other, less trivial kneading sequences lead to values of α between these two extremes. We note, however, that it is only the infinite "tail" of the sequence that determines the asymptotic scaling behavior. The number of sequences leading to the same singularity α may be simply found, and leads via Eq. (2.30) to exactly the same results for $f(\alpha)$ as the partition-function analysis above.

Finally, in Fig. 4 we display the curve $f(\alpha)$. The curve has been obtained for $l_1=0.25$, $l_2=0.4$ and $p_1=0.6$, $p_2=0.4$. The leftmost point on the curve is $f=0$, $\alpha=\ln(0.6)/\ln(0.25)$. This is the value that in Eqs. (2.31) and (2.33) obtains for $n=m$. At any level of the construction there is exactly one such segment ($f=0$) and the singularity is

$$\ln p_1/\ln l_1 = \mathrm{Inf}\{\ln p_1/\ln l_1, \ln p_2/\ln_2\} .$$

This value of α is also D_{∞}. The rightmost point on the graph again corresponds to $f=0$, but now

$$\alpha = \ln p_2/\ln l_2 = \mathrm{Sup}\{\ln p_1/\ln l_1, \ln p_2/\ln l_2\} .$$

This is also $D_{-\infty}$. Whereas D_{∞} corresponds to the region in the set where the measure is most concentrated, $D_{-\infty}$ corresponds to that where the measure is most rarefied. For $q=0$ we simply obtain $f=D_0$, where D_0 is the Hausdorff dimension of the set. This is the maximum of the graph $f(\alpha)$.

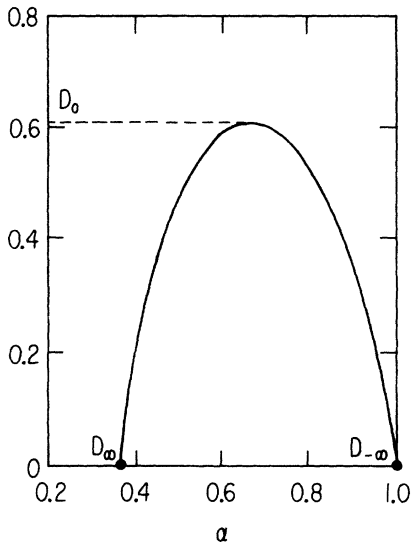

FIG. 4. The plot of f vs α for the set in Fig. 2. Note that $f=0$ corresponds to α values $D_{-\infty}=\ln(0.4)/\ln(0.4)=1.0$ and $D_{\infty}=\ln(0.6)/\ln(0.25)=0.3684$.

Certain features of this curve are quite general, and follow from Eqs. (1.9)–(1.12). From Eq. (1.9) we find immediately that

$$\frac{\partial f}{\partial \alpha} = q , \tag{2.35a}$$

$$\frac{\partial^2 f}{\partial \alpha^2} < 0 . \tag{2.35b}$$

Thus, for any measure the curve $f(\alpha)$ will be convex, with a single maximum at $q=0$, and with infinite slope at $q=\pm\infty$. Also from Eq. (1.10) with $q=1$, we find that $\alpha(1)=f(1)$. The slope $\partial f/\partial\alpha$ there is unity. This general behavior of the curve $f(\alpha)$ will be seen in all cases where the measure possesses a continuous spectrum.

Although this example is rather simple, it contains many of the properties of the richer sets considered in Sec. III. In particular, we will not lose this intuitive view of the meaning of α and f.

5. *Other types of spectra*

We can obtain more insight into the meaning of the f-α spectrum for a measure by considering two examples of measures on continuous supports. Many of the most interesting measures encountered in applications lie on continuous supports, including the growth measure for diffusion-limited aggregates and strange attractors for systems of ordinary differential equations.

The first example is a simple generalization of the two-scale Cantor set defined by (2.24). A unit interval is subdivided into three segments, two of length l_2 and one of length l_1. The two former intervals each receive a proportion of the total measure given by p_2, and the latter interval receives a proportion given by p_1. We imagine that $l_1+2l_2=1$ and that $p_1+2p_2=1$. We also imagine, for the sake of the argument below, that $p_2/l_2>p_1/l_1$ and that $l_2>l_1$. Each of these three intervals is then subdivided in the same manner, and so forth. Although the measure on the line segment is rearranged at each step of the recursive process, the support for the measure remains at each step the original line segment. Thus we expect that D_0 for this measure will be 1. Furthermore, the densest intervals on the line segment contract not to one point (as was the case in the two-scale Cantor set), but to a set of points of finite dimension. Thus, we expect the lowest value of α, and hence the value of D_∞, to correspond to a nonzero value of f. Note that there is always only one segment at the lowest value of the density, so that we still expect $D_{-\infty}$ to correspond to a value of $f=0$. The condition (2.18) above on Γ requires that

$$\Gamma(q,\tau,l_2)=\frac{p_1^q}{l_1^\tau}+2\frac{p_2^q}{l_2^\tau}=1\ . \tag{2.36}$$

The solution is simple and is displayed in Fig. 5. As predicted above, $f(q\to\infty)\neq 0$, so that the leftmost part of the f-α curve resembles a hook.

The second example is a set generated according to a different rule than the Cantor sets. The method is displayed in Fig. 6. At each stage, only the regions which

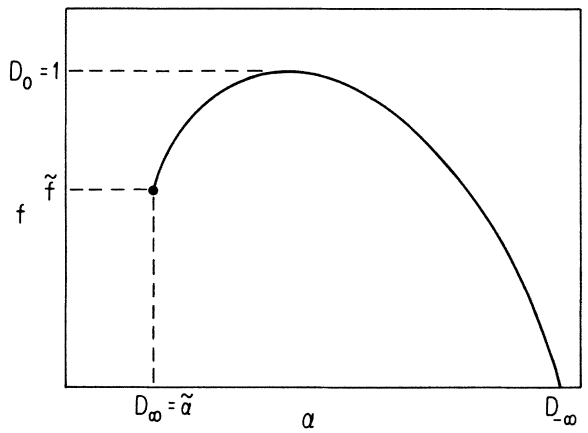

FIG. 5. The function $f(\alpha)$ for the measure defined by Eq. (2.36). Note that D_∞ corresponds to a nonzero value of f. Also, $D_0=1$.

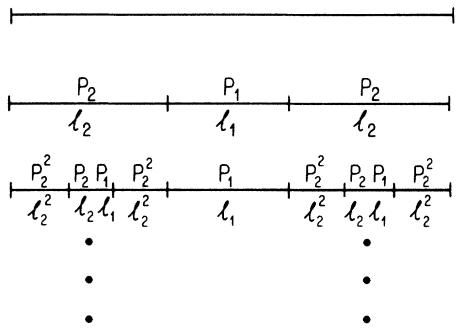

FIG. 6. The partitioning process for the measure yielding the partition function (2.37). Only those segments receiving a measure multiplied by p_2 at any stage of the construction are further subdivided. This measure is far less self-similar than those generated by the Cantor process.

have had their measure multiplied by a factor p_2 in the preceding stage are subdivided further, while the regions which have had their measure multiplied by a factor p_1 are not subdivided further. Thus the expression for the measure density of any region, at any stage of the iterative construction, will have, at most, one factor of p_1. The measure generated by this construction is much less self-similar than that considered in Sec. III C 4. For this measure the partition function is given for large n by

$$\Gamma(q,\tau,l_2^n)=(p_1^q/l_1^\tau)\Gamma^U(l_2^{n-1})+2(p_2^q/l_2^\tau)\Gamma(l_2^{n-1})\ , \tag{2.37}$$

where Γ^U is the partition function for a uniform measure on a line segment. It is easy to show that

$$\tau(q)=\min\{q-1,q\tilde{\alpha}-\tilde{f}\}\ , \tag{2.38}$$

with $\tilde{\alpha}=\ln(p_2)/\ln(l_2)$, and $\tilde{f}=\ln(\frac{1}{2})/\ln(l_2)$. This example corresponds to a discrete, rather than a continuous, f-α curve, consisting of a point at $(\tilde{\alpha},\tilde{f})$ and a point at (1,1). This result should not surprise us, as this measure is properly described as a nonsingular background interrupted by singularities upon a Cantor set of dimension $\tilde{f}$.

III. EXAMPLES FROM DYNAMICAL SYSTEMS

In this section we examine the implications of the formalism of Sec. II for three examples: (i) the 2^∞ cycle at the accumulation point of period doubling, (ii) the set of irrational winding numbers at the onset of chaos via quasiperiodicity, and (iii) the critical cycle elements at the golden-mean winding number for the same problem. In all cases we calculate numerically the D_q, and use Eqs. (1.10) and (1.11) to extract $\alpha(q)$, $f(q)$, and a plot of $f(\alpha)$. In all three cases we can find theoretically $D_\infty, D_{-\infty}$, and thus $\alpha(q=\pm\infty)$.

A. The 2^∞ cycle of period doubling

Dynamical systems that period double on their way to chaos can be represented by one-parameter families of maps $M_\lambda(\mathbf{x})$, where M_λ: $R^F\to R^F$, and F is the number of degrees of freedom. At values of $\lambda=\lambda_n$ the system

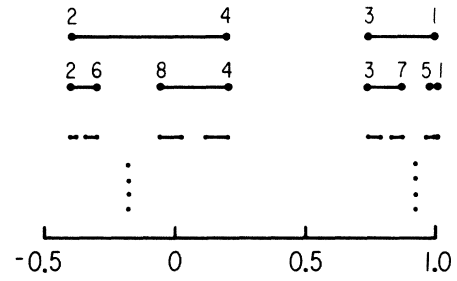

FIG. 7. The construction of the period-doubling attractor; the indices refer to the number of the iterate of $x=0$. The lines represent the scales l_i. Note the similarity with Fig. 2.

gains a stable 2^n-periodic orbit. This period-doubling cascade accumulates at λ_∞, where the system possesses a 2^∞ orbit. We generated numerically the set of elements of this orbit for the map $x'=\lambda(1-2x^2)$, with $\lambda_\infty \approx 0.837\,005\,134\ldots$.[15] The points making up the cycle are displayed in Fig. 7. The iterates of $x=0$ form a Cantor set, with half the iterates falling between $f(0)$ and $f^3(0)$ and the other half between $f^2(0)$ and $f^4(0)$. The most natural partition, $\{S_i\}$, for this case simply follows the natural construction of the Cantor set as shown in Fig. 7. At each level of the construction of this set, each l_i is the distance between a point and the iterate which is closest to it. The measures p_i of these intervals are all equal.

With 2^{11}-cycle elements we solved numerically $\Gamma=1$, thereby generating the D_q-versus-q curve shown in Fig. 8. From these results we calculated $\alpha(q)$ from Eq. (1.11) and $f(\alpha)$ from (1.10). The curve $f(\alpha)$ is displayed in Fig. 9.

To understand the shape of the curve in Fig. 9 we first consider the end points of the curve (for which $f=0$). As with the example solved in Sec. II C 4, we expect these two points to be determined by the most rarefied and the most concentrated intervals in the set. As has been shown by Feigenbaum,[15] these have scales $l_{-\infty}\sim\alpha_{\rm PD}^{-n}$ and $l_{+\infty}\sim\alpha_{\rm PD}^{-2n}$, respectively, where $\alpha_{\rm PD}=2.502\,907\,875\ldots$ is the universal scaling factor.[15] Since the measures there

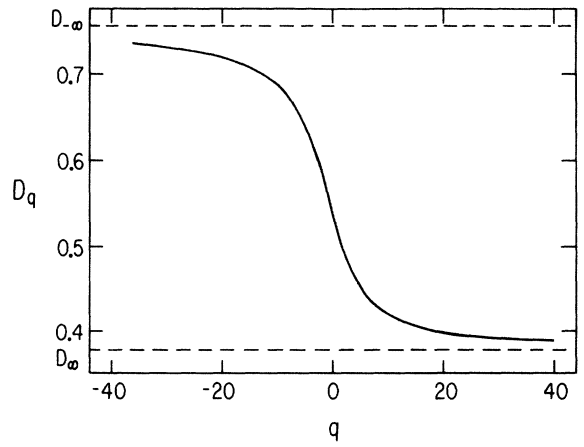

FIG. 8. D_q vs q calculated for the period-doubling attractor of Fig. 7.

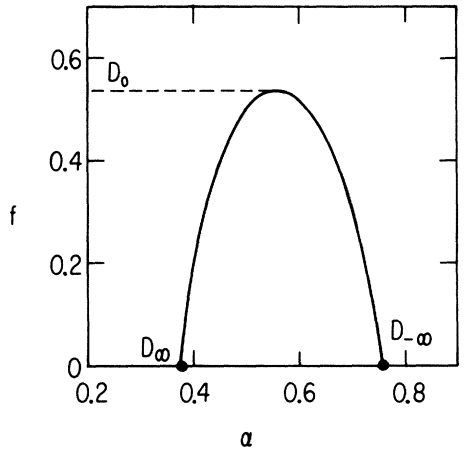

FIG. 9. The function $f(\alpha)$ for the period-doubling attractor of Fig. 7.

are simply $p_{-\infty}\sim 2^{-n}$, we expect these end points to be $\ln p_{-\infty}/\ln l_{-\infty}$ and $\ln p_\infty/\ln l_\infty$, respectively. These values are also $D_{-\infty}$ and D_∞, so that we find

$$D_{-\infty}=\frac{\ln 2}{\ln\alpha_{\rm PD}}=0.755\,51\ldots, \tag{3.1a}$$

$$D_\infty=\frac{\ln 2}{\ln\alpha_{\rm PD}^2}=0.377\,75\ldots. \tag{3.1b}$$

These values are in extremely good agreement with the numerically determined endpoints of the graph. The curve $f(\alpha)$ is perfectly smooth. The maximum is at $D_0=0.537\ldots$, in agreement with previous calculations of the Hausdorff dimension for this set. Since the slope of the curve $f(\alpha)$ is q, $\alpha(q)$ will be very close to $D_{\pm\infty}$ even for $|q|\sim 10$. However, Fig. 8 indicates that D_q is far from converged to $D_{\pm\infty}$ even for $q\sim\pm 40$. Thus, the transformations (1.10) and (1.11) lead more easily to good estimations of $D_{\pm\infty}$ than do direct calculations of the D_q's.

B. Mode-locking structure

Dynamical systems possessing a natural frequency ω_1 display very rich behavior when driven by an external frequency ω_2. When the "bare" winding number $\Omega=\omega_1/\omega_2$ is close to a rational number, the system tends to mode lock. The resulting "dressed" winding number, i.e., the ratio of the response frequency to the driving frequency, is constant and rational for a small range of the parameter Ω. At the onset of chaos the set of irrational dressed winding numbers is a set of measure zero, which is a strange set of the type discussed above. The structure of the mode locking is best understood in terms of the "devil's staircase" representing the dressed winding number as a function of the bare one. Such a staircase is shown in Fig. 10 as obtained for the map[16,17]

$$\theta_{n+1}=\theta_n+\Omega-\frac{K}{2\pi}\sin(2\pi\theta_n)\,, \tag{3.2}$$

with $K=1$, which is the onset value above which chaotic orbits exist.

To calculate $D_{\pm\infty}$ analytically we make use of previous findings that the most extremal behaviors of this staircase are found at the golden-mean sequence of dressed winding numbers

$$F_n/F_{n+1}\to w^*=(\sqrt{5}-1)/2\approx 0.6108\ldots,$$

where F_n are the Fibonacci numbers, ($F_0=0$, $F_1=1$, and $F_n=F_{n-1}+F_{n-2}$ for $n\geq 2$) and at the harmonic sequence $1/Q\to 0$.[16,17] The most rarefied region of the staircase is located around the golden mean. Shenker found that the length scales l_i vary in that neighborhood as $l_{-\infty}\sim F_n^{-\delta}\sim(w^*)^{n\delta}$, where $\delta=2.1644\ldots$ is a universal number.[18] The corresponding changes in dressed winding number are

$$p_{-\infty}\sim F_n/F_{n+1}-F_{n+1}/F_{n+2}\sim(w^*)^{2n}.$$

We thus conclude that

$$D_{-\infty}=\frac{\ln p_{-\infty}}{\ln l_{-\infty}}=\frac{2}{\delta}=0.9240\ldots. \tag{3.3a}$$

For the $1/Q$ series it has been shown that changes in dressed winding number go as the square root of changes in bare winding number, i.e., that $p_i\sim l_i^{1/2}$.[16] This series determines the most concentrated portion of the staircase (Fig. 10), which means that $p_\infty\sim l_\infty^{1/2}$, leading to

$$D_\infty=\ln p_\infty/\ln l_\infty=\tfrac{1}{2}. \tag{3.3b}$$

To construct the curve $f(\alpha)$ we generated 1024 mode-locked intervals following the Farey construction, which also defines the partition $\{S_i\}$.[17] For each two neighboring intervals (see Fig. 10) we measured the change both in bare and in dressed winding numbers. The changes in bare winding numbers determined the scales l_i of the partition $\{S_i\}$, whereas the changes in dressed winding numbers were defined to be the measures p_i. Solving then the equation $\Gamma=1$ we generated D_q as shown in Fig. 11 (for $q>0$ we accelerated the convergence as will be described shortly). Figure 12 shows $f(\alpha)$ for this case. Again the curve is smooth, in contrast to scaling functions found for

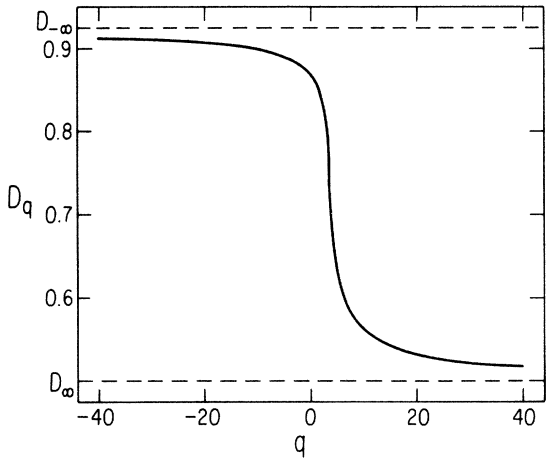

FIG. 11. D_q vs q for the staircase of Fig. 10.

the same problem by other authors.[15,21] Note that the maximum on Fig. 12 gives the fractal dimension D_0 of the mode-locking structure as $D_0\approx 0.87\ldots$, in agreement with the predictions of Refs. 16 and 17. The rightmost branch of the curve $f(\alpha)$ in Fig. 12 (i.e., for $q<0$) converges vary rapidly within the Farey partition. This is, however, not the case for the leftmost branch (i.e., for $q>0$). To improve the convergence of this portion of the curve substantially, we made use of the following trick. In general, the partition function (2.1) will be of the form

$$\Gamma(l)=ae^{\gamma\ln l}, \tag{3.4}$$

where a and γ are constants. The convergence is often slowed down by the prefactor a and by the logarithmic dependence on l. However, by considering instead the ratio

$$\frac{\Gamma(l)}{\Gamma(2l)}=e^{-\gamma\ln 2}, \tag{3.5}$$

we find that a and l do not appear in the equation. We thus determine $\tau(q)$ by requiring that

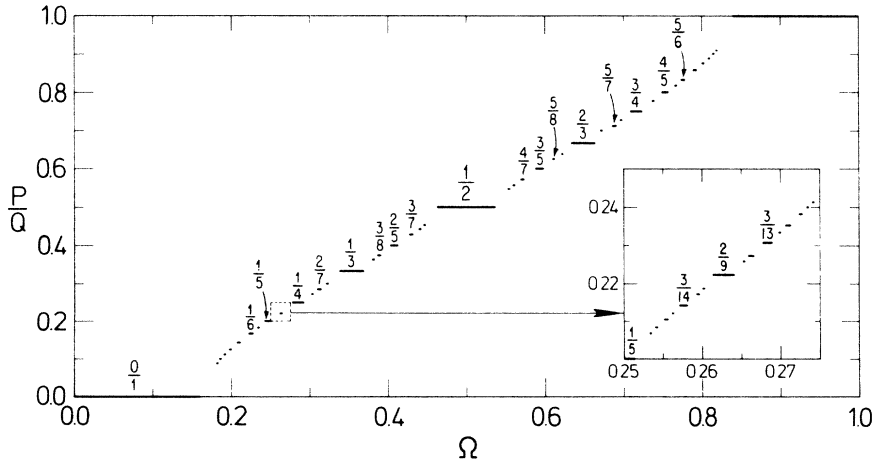

FIG. 10. The "devil's staircase" for the critical circle map of Eq. (3.2). The "dressed" winding number is plotted vs the "bare" winding number (Ref. 16).

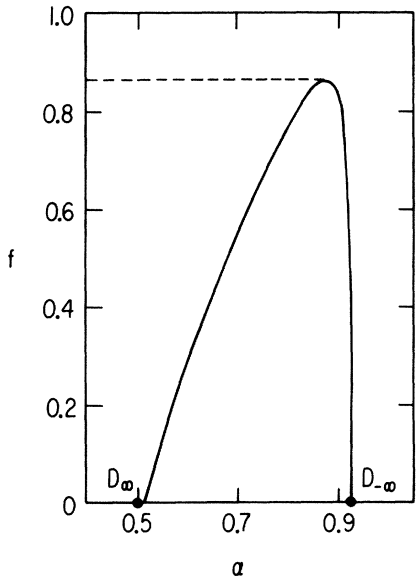

FIG. 12. A plot of f vs α for the mode-locking structure of the circle map. The left portion of the curve is found by accelerated convergence as described in Sec. III B.

$$\frac{\Gamma(l)}{\Gamma(2l)}(\tau,q)=1 .$$

In general, the denominator can be chosen to be of the form $\Gamma(bl)$, where b is a constant. The leftmost portion of the curve was generated with this method by calculating $\Gamma(l(1452))/\Gamma(l(886))=1$ [where $l(1452)$ and $l(886)$ are the maximal scales for partitions with 1452 and 886 intervals, respectively], and we observe that it passes through the point $(D_\infty,0)$. We found empirically that this method usually did not give reliable results for large values of $|q|$. Still, this method did successfully generate the entire curve in Fig. 12. We emphasize the ease of this measurement. The rightmost branch of the f-α curve of Fig. 12 converges very rapidly, even when only 8—16 mode-locked intervals are available.

C. Quasiperiodic trajectories for circle maps

Circle maps of the type (3.1) exhibit a transition to chaos via quasiperiodicity. A well-studied transition takes place at $K=1$ with dressed winding number equal to the golden mean, w^*. [18–20] We have at this point studied the structure of the trajectory $\theta_1,\theta_2,\ldots,\theta_i,\ldots$. To perform the numerical calculation we chose $\theta_1=f(0)$ and truncated the series θ_i at $i=2584=F_{17}$. The distances $l_i=\theta_{i+F_{16}}-\theta_i$ (calculated mod 1) define natural scales for the partition with measures $p_i=1/2584$ attributed to each scale. Figure 13 shows D_q versus q calculated for this set and Fig. 14 shows the corresponding function $f(\alpha)$. Again the curve is smooth. Shenker found for this problem that the distances around $\theta\sim 0$ scale down by a universal factor $\alpha_{\rm GM}=1.288\,5\ldots$ when the trajectory θ_i is truncated at two consecutive Fibonacci numbers,

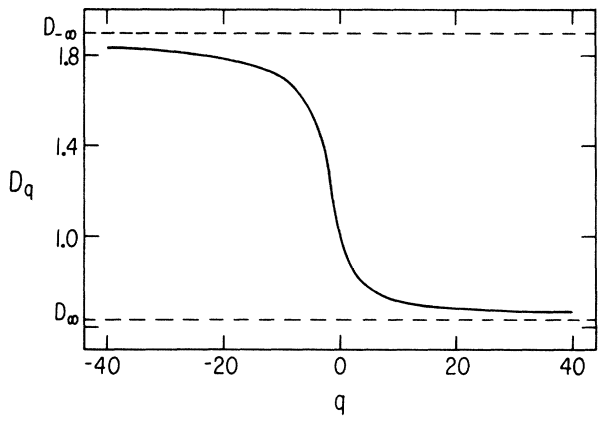

FIG. 13. D_q plotted vs q for the critical trajectory of a circle map with golden-mean winding number.

F_n,F_{n+1}.[18] This corresponds to the most rarefied region so that $l_{-\infty}\sim\alpha_{\rm GM}^{-n}$. The corresponding measure scales as $p_{-\infty}\sim 1/F_n\sim(\omega^*)^n$, leading to

$$D_{-\infty}=\frac{\ln w^*}{\ln\alpha_{\rm GM}^{-1}}=1.898\,0\ldots . \tag{3.6a}$$

The map (3.2) for $K=1$ has at $\theta=0$ a zero slope with a cubic inflection and is otherwise monotonic. The neighborhood around $\theta=0$, which is the most rarefied region of the set, will therefore be mapped onto the most concentrated region of the set. As the neighborhood around $\theta=0$ scales as $\alpha_{\rm GM}$ when the Fibonacci index is varied, the most concentrated regime will scale as $\alpha_{\rm GM}^3$ due to the cubic inflection. This means that $l_\infty=\alpha_{\rm GM}^{-3n}$ and $p_\infty=(w^*)^n$, so that we obtain

$$D_\infty=\frac{\ln w^*}{\ln\alpha_{\rm GM}^{-3}}=0.632\,6\ldots . \tag{3.6b}$$

Figure 14 shows that the curve passes very close to the points $(D_\infty,0)$ and $(D_{-\infty},0)$. Again, however, we find

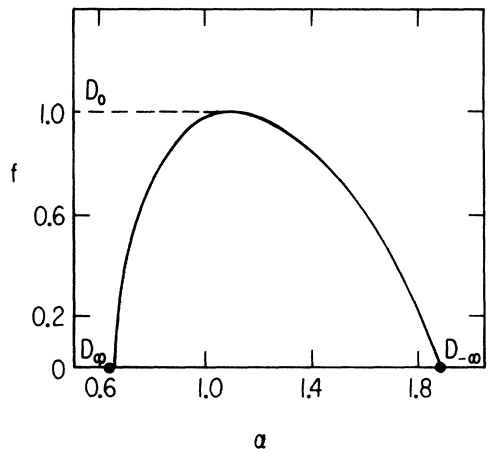

FIG. 14. A plot of f vs α for the golden-mean trajectory for the circle map.

that the dimensions D_q are far from $D_{\pm\infty}$ even for $q\sim\pm 40$.

To check for universality it is important to investigate $f(\alpha)$ for a higher-dimensional version of a circle map. We chose the dissipative standard map,

$$\theta_{n+1}=\theta_n+\Omega+br_n-\frac{K}{2\pi}\sin(2\pi\theta_n)\ ,$$
$$r_{n+1}=br_n-\frac{K}{2\pi}\sin(2\pi\theta_n)\ , \tag{3.7}$$

and studied the critical cycle for $b=0.5$, again truncated at $i=2584=F_{17}$. We defined the scales by the Euclidean distances

$$l_i=[(\theta_{i+F_{16}}-\theta_i)^2+(r_{i+F_{16}}-r_i)^2]^{1/2}\ . \tag{3.8}$$

We found that the convergence for the two-dimensional (2D) case was slightly slower than for the one-dimensional (1D) case. This is, however, to be expected since it was found by Feigenbaum, Kadanoff, and Shenker that the convergence of the scaling number $\alpha_{\rm GM}$ is slower for the 2D case than for the 1D case.[19] To improve the convergence we again made use of the ratio trick as embodied in Eqs. (3.4) and (3.5). For this case we calculated the partition function for two consecutive Fibonacci numbers, $F_{16}=1597$ and $F_{17}=2584$, and found τ from the requirement

$$\frac{\Gamma(l(F_{17}))}{\Gamma(l(F_{16}))}(\tau,q)=1$$

[$l(F_i)$ are the maximal scales for the partitions]. This improves the convergence significantly, and the f-α curve for this 2D case coincides almost completely with the curve found for the 1D case and displayed in Fig. 14.

IV. CONCLUSION

Most previous characterizations of strange sets arising in physics have followed the example of critical phenomena in relying upon a few universal numbers to characterize the physical systems generating these sets. Thus, strange attractors are characterized by their Hausdorff dimensions, or by the scaling exponents of particularly divergent regions of their measure. However, these numbers reflect only a small part of the universal scaling structure of these systems. Feigenbaum introduced scaling functions in order to describe the complex scaling properties of attractors at the onset of chaos.[15] These scaling functions contain all of the geometric information about the attractor, in contrast to the partial information furnished by local scaling exponents. These functions are, however, nowhere differentiable, and are thus very difficult to use. The full complexity of this scaling structure is more conveniently reflected by the continuous spectrum of exponents α and their densities $f(\alpha)$, of which previously investigated scaling exponents and Hausdorff dimensions comprise only a part.

Not only does this spectrum enrich our conceptual vocabulary, it should enrich our experimental vocabulary as well. The numerical studies of Sec. III were straightforward and did not require large investments of computer time in order to obtain extremely accurate results. Furthermore, this spectrum can be measured, and has been measured, in experiments upon physical realizations of dynamical systems.[23] The measurement of this spectrum should result in new tests of scaling theories of nonlinear systems.

ACKNOWLEDGMENTS

We would like to thank P. Jones and J. Rudnick for stimulating discussions. This work was supported by the U.S. Office of Naval Research, by the National Science Foundation through Grant No. DMR-83-16626, and through the Materials Research Laboratory of the University of Chicago. One of us (I.P.) wishes to thank Professor S. Berry for his warm hospitality and also acknowledge the support of the Minerva Foundation (Munich, West Germany).

---

*Permanent address: Department of Chemical Physics, The Weizmann Institute of Science, 76100 Rehovot, Israel.

†Present address: AT&T Bell Laboratories, 600 Mountain Avenue, Murray Hill, NJ 07974.

[1]R. Bowen, *Equilibrium States and the Ergodic Theory of Anisov Diffeomorphisms,* Vol. 470 of *Lectures Notes in Mathematics* (Springer, Berlin, 1975); M. Widom, D. Bensimon, L. P. Kadanoff, and Scott J. Shenker, J. Stat. Phys. **32**, 443 (1983).

[2]I. Procaccia, in Proceedings of the Nobel Symposium on Chaos and Related Problems [Phys. Scr. T **9**, 40 (1985)].

[3]K. G. Wilson, Sci. Am. **241**, (2) 158 (1979).

[4]B. B. Mandelbrot, Ann. Isr. Phys. Soc. **225** (1977); H. Aref and E. D. Siggia, J. Fluid Mech. **109**, 435 (1981).

[5]I. Procaccia, J. Stat. Phys. **36**, 649 (1984).

[6]L. de Arcangelis, S. Redner, and A. Coniglio, Phys. Rev. B **31**, 4725 (1985).

[7]T. A. Witten, Jr. and L. M. Sander, Phys. Rev. Lett. **47**, 1400 (1981).

[8]T. C. Halsey, P. Meakin, and I. Procaccia (unpublished).

[9]B. Widom, J. Chem. Phys. **43**, 3892 (1965); M. E. Fisher, in Proceedings of the University of Kentucky Centennial Conference on Phase Transitions (March 1965) (unpublished); A. Z. Patashinskii and V. L. Prokovskii, Zh. Eksp. Teor. Fiz. **50**, 439 (1966) [Sov. Phys.—JETP **23**, 292 (1966)]; L. P. Kadanoff, W. Gotze, D. Hamblen, R. Hecht, E. A. S. Lewis, V. V. Palciauskas, M. Rayl, J. Swift, D. Aspnes, and J. Kane, Rev. Mod. Phys. **39**, 395 (1967).

[10]L. P. Kadanoff, Physics **2**, 263 (1966).

[11]In fact, for many two-dimensional critical phenomena we know [see, for instance, D. Friedan, Z. Qiu, and Stephen Shenker, Phys. Rev. Lett. **52**, 1575 (1984)] that there is only a finite set of dist t y's.

[12]L. Turkevich and H. Scher, Phys. Rev. Lett. **55**, 1024 (1985).

[13]H. G. E. Hentschel and I. Procaccia, Physica **8D**, 435 (1983).

[14]P. Grassberger and I. Procaccia, Physica **13D**, 34 (1984).

[15]M. J. Feigenbaum, J. Stat. Phys. **19**, 25 (1978); **21**, 669 (1979).

See also the two reprint compilations: P. Cvitanović, *Universality in Chaos* (Hilger, Bristol, 1984); Hao Bai-lin, *Chaos* (World Scientific, Singapore, 1984).

[16]M. H. Jensen, P. Bak, and T. Bohr, Phys. Rev. Lett. **50**, 1637 (1983); Phys. Rev. A **30**, 1960 (1984); **30**, 1970 (1984).

[17]P. Cvitanović, M. H. Jensen, L. P. Kadanoff, and I. Procaccia, Phys. Rev. Lett. **55**, 343 (1985).

[18]Scott J. Shenker, Physica **5D**, 405 (1982).

[19]M. J. Feigenbaum, L. P. Kadanoff, and Scott J. Shenker, Physica **5D**, 370 (1982).

[20]S. Ostlund, D. Rand, J. P. Sethna, and E. D. Siggia, Phys. Rev. Lett. **49**, 132 (1982); Physica **8D**, 303 (1983).

[21]P. Cvitanović, B. Shraiman, and B. Soderberg (unpublished).

[22]A. Cohen and I. Procaccia, Phys. Rev. A **31**, 1872 (1985), and references therein.

[23]M. H. Jensen, L. P. Kadanoff, A. Libchaber, I. Procaccia, and J. Stavans, Phys. Rev. Lett. **55**, 2798 (1985).